Article

Numerical Study of Aerodynamic Characteristics of Axial Fans with Different Blade Configurations

Mehrab Hasan [1*],

[1] University of Oklahoma,Norman,Oklahoma;MehrabHasan@my.unt.edu

Abstract

The influence of blade number on axial fan aerodynamic performance is a critical factor in optimizing fan design for industrial applications. This study presents a comparative analysis of five-blade and seven-blade axial fan configurations based on the conventional RS 1442047 model specifications. Three-dimensional fan geometries were developed in SOLIDWORKS and subsequently imported into ANSYS for numerical simulation. The governing equations were solved using a pressure-based transient solver employing the SIMPLE algorithm with second-order upwind discretization. Simulations were performed at different inlet air velocities of 2.5, 5, and 7.5 m/s with a constant rotational speed of 4600 rpm. The results demonstrated that static pressure increased proportionally with inlet velocity for both configurations, with the seven-blade fan consistently generating higher static pressure than the five-blade counterpart across all operating conditions. At the maximum tested velocity of 7.5 m/s, the seven-blade fan achieved a maximum static pressure of 53.65 Pa compared to 48.91 Pa for the five-blade design. However, both configurations exceeded the allowable static pressure limit of 24.909 Pa at this velocity, indicating potential operational constraints. The findings suggest that while additional blades enhance pressure generation capability, inlet velocities beyond 5 m/s may compromise long-term fan performance and reliability.

Keywords: Axial Fan, CFD, SIMPLE, Static Pressure

1. Introduction

Axial fans are extensively employed across wide range of engineering applications, including industrial ventilation, air conditioning systems, electronic cooling [1]. These turbomachines operate on the fundamental principle of airflow deflection, where the rotating blades impart kinetic energy to the air, generating both axial and tangential velocity components[2]. While axial fans are incapable of developing high pressures comparable to centrifugal designs, they excel at handling substantial air volumes at relatively low pressures, making them indispensable for numerous industrial applications [2].

The advancement of Computational Fluid Dynamics (CFD) has revolutionized the design and optimization of axial fans. Since the 1980s, CFD methods have provided alternative approaches to fan flow analysis, enabling engineers to predict performance curves and inspect inter-blade flow patterns with unprecedented detail [3]. Extensive research has been carried out on the performance optimization and development of axial fans, on blade number optimization. Research on blade number optimization has received considerable attention in recent literature. Liu et al. conducted finite element analysis on mining axial fans with 8, 9, and 10 blades, investigating the relationship between blade quantity and pressure distribution within the fluid domain. Their study revealed that the number of blades becomes a crucial factor affecting fan performance, as the work done by blades on the airflow directly influences air exchange efficiency [4]. Similarly, Podgaietsky et al. performed sensitivity analysis on key design parameters including number of blades, pitch angle, chord length,

and airfoil characteristics, establishing relationships between these parameters and overall fan efficiency[5].

The optimization of blade geometry has been extensively studied for improving aerodynamic performance. Research in mine ventilation fans by Panigrahi and Mishra demonstrated that angle of attack significantly affects lift and drag coefficients, with stall conditions typically occurring at angles between 12° and 15°[6]. Their CFD simulations at Reynolds number, $Re = 3 \times 10^6$ provided criteria for selecting efficient blade profiles based on lift-to-drag ratios.

Static pressure distribution analysis remains a primary metric for characterizing axial fan performance. Liu et al. further demonstrated that prediction deviations using improved CFD methods could be reduced to as little as 3% compared to conventional approaches, representing significant improvements in simulation accuracy [3].

The SIMPLE (Semi-Implicit Method for Pressure-Linked Equations) algorithm, developed by Patankar and Spalding, has become the standard pressure-velocity coupling approach for incompressible flow simulations[7]. This iterative procedure derives a pressure equation by introducing the momentum equation into mass balance, then updates velocity fields based on new pressure values. Variations including SIMPLER and SIMPLEC have been developed to enhance convergence rates, with SIMPLEC particularly effective for problems where pressure-velocity coupling is the primary convergence deterrent [8]. Razib et al. used SIMPLE algorithm for the collocated arrangement of scalar and vector variables to solve the equations expressed in Cartesian velocity components and applied that to assess pressure distributions on the surface of the NACA 0012 hydrofoil at different angles of attack[9].

Recent studies have also explored noise reduction strategies alongside aerodynamic optimization. Ocker et al. investigated slitted leading edge designs for flat-plate axial fans, demonstrating that such modifications can reduce turbulence interaction noise across broad frequency ranges[10]. Qi et al. proposed wavy blade configurations that achieved noise reductions of 1.5-2.6 dB while maintaining acceptable aerodynamic performance, establishing that the primary noise reduction mechanism involves transformation of layered vortex structures into uncorrelated comb vortex patterns [11].

Previously, Hemant Kumawat , analyzed and simulated results for fans having seven to eleven blades and he plotted static pressure, and temperature contour for those fans[2]. He finally determined that fan with eleven blades had the highest efficiency at air velocity of 22 m/s . Also, Thumbe et al. conducted an analysis of axial fan having six blades. Jain and Deshpande analyzed the airflow distribution from a radial axial flow fan and considered 1680 rpm and 25.26 kg/s as the input conditions for their analysis[12].

The present study builds upon this foundation by analyzing five-blade and seven-blade axial fan configurations for the RS 1442047 model [13]. Static pressure and velocity streamline distributions are investigated across variable inlet velocity conditions, with the objective of characterizing the aerodynamic performance differences attributable to blade number variation at high rotational speeds.

2. Methodology

The numerical investigation followed a systematic CFD workflow beginning with geometry creation, where the five blade and seven blade axial fan models were designed in SOLIDWORKS based on the RS 1442047 product data sheet specifications and subsequently imported into ANSYS for analysis. A computational domain extending 40 mm in the x and y directions, 30 mm upstream, and 200 mm downstream was constructed to adequately capture the inlet and outlet flow characteristics. Boundary conditions included inlet air velocities of 2.5, 5, and 7.5 m/s , zero gauge pressure at the outlet, and an angular velocity of 4600 rpm applied to the fan zone through mesh motion. The SIMPLE algorithm was used to solve the governing equations iteratively until

convergence. Post-processing involved extraction of static pressure contours on blade surfaces and velocity streamlines within the flow domain, facilitating a direct aerodynamic comparison between the two fan configurations. Following flow chart demonstrates a detailed breakdown of the procedures (Figure 1).

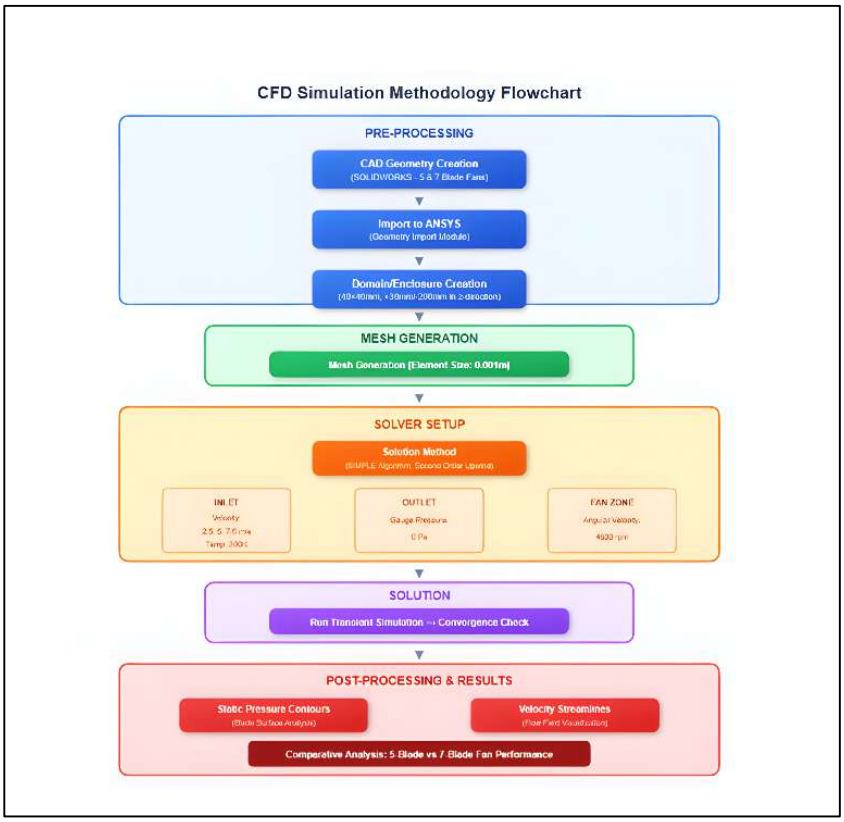

Figure 1. Workflow diagram of the analysis procedures.

2.2. Geometry and CFD Model

The geometry was created from the dimensions provided by the catalogue of RS PRO DC Axial Fan. The frame is rectangular in shape, and it is 50x50x10 mm in dimension. For mesh cell number constraints in ANSYS student version software, a simplified geometry of the fan was created. Then it was imported into ANSYS and modeled. To observe the physical properties, a domain was created using enclosure module. The enclosure was 40 mm in x and y directions, 30 mm in positive z direction and 200 mm in negative z directions. These dimensions were chosen for better observation. As per the product datasheet [13], the angular velocity for the fan was determined at 4600 rpm and all the simulations were conducted at this motion.

2.3. Simulation Conditions

A pressure based transient simulation method was adopted for this study. For model, k- ε model was selected. The model was selected as realizable. For near wall treatment, scalable wall function was used. For Solution, SIMPLE algorithm and second order upwind method were used. SIMPLE algorithm is an iterative procedure, and it starts with an initial guess value and continues to run until it converged.

2.4. Domain Size and Mesh

For mesh, three named selections were created as inlet, outlet, and wall. Element size was selected as 0.001m and program-controlled element was chosen. Due to mesh cell number limitations, much smaller mesh element size was not selected. For both seven blade and five blade fans, same setup was used. Quality of mesh was selected as smooth. Mesh element number for five blade fan was 293334 and for seven blade fan it was 319240. The surface mesh generation was demonstrated for five blade fan in Figure 2.

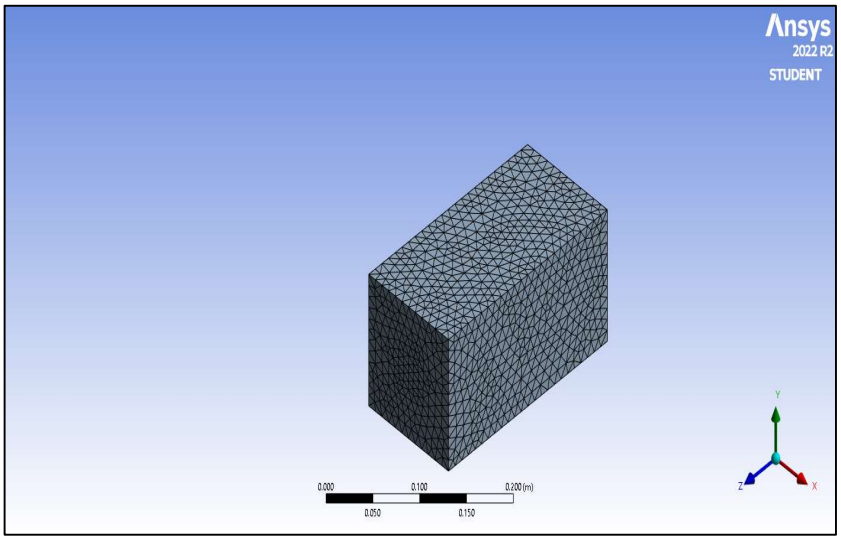

Figure 2. Surface Mesh of five blade fan.

2.5 Governing Equations and Discretization Schemes

2.5.1 Continuity Equation

The continuity equation (Eq. 1) represents the conservation of mass within the computational domain surrounding the axial fan[14]. This equation states that the rate of change of density plus the divergence of mass flux must equal zero, ensuring that air mass is neither created nor destroyed during the simulation. For the five-blade and seven-blade fan configurations analyzed in this study, the continuity equation guarantees that the volumetric flow rate entering through the inlet boundary equals the flow exiting at the outlet, which is essential for accurate prediction of fan performance characteristics. All the symbols used in the equation are elaborated in Table 1.

$$\frac{\partial \rho}{\partial t} + \nabla \cdot \left(\rho \vec{V}\right) = 0 \quad (1)$$

Table 1. Nomenclature

Symbols	Meaning
P	Pressure
μ	Viscosity
ρ	Density
T	Temperature
K	Thermal conductivity
H	Enthalpy
$\vec{V}$	Velocity vector
$\vec{f}$	Body force per unit mass
Ø	Dissipation function
$\bar{\bar{\tau}}$	Viscous stress tensor
τ_{ij}	Stress tensor component

2.5.2 Momentum Equation

The momentum equation (Eq. 2), derived from Newton's second law, governs the relationship between fluid acceleration and the forces acting on air particles flowing through the fan [12]. The equation accounts for pressure gradients responsible for static pressure rise across the blades, viscous stresses that influence boundary layer development on blade surfaces, and body forces. For the rotating fan operating at 4600 rpm, mesh motion was applied to incorporate Coriolis and centrifugal effects, enabling accurate prediction of the pressure distribution differences observed between the five-blade and seven-blade configurations at inlet velocities of 2.5, 5, and 7.5 m/s .

$$\rho \frac{D\vec{V}}{Dt} = -\nabla p + \nabla \cdot \bar{\bar{\tau}} + \rho \vec{f} \tag{2}$$

2.5.3 Energy Conservation Equation

The energy conservation equation (Eq. 3) describes the transport of enthalpy, pressure work, heat conduction, and viscous dissipation within the flow domain [15]. The dissipation function φ (Eq. 4) quantifies the irreversible conversion of mechanical energy to thermal energy due to viscous stresses, particularly in high-shear regions near blade surfaces. Under the isothermal conditions (300K) employed in this study, thermal effects on fan performance remained negligible. The governing equations were solved using the SIMPLE algorithm [7]. These equations are applicable for both compressible and incompressible fluids and are presented in conservative form.

$$\rho \left[\frac{\partial h}{\partial t} + \nabla \cdot \left(h\vec{V}\right)\right] = -\frac{Dp}{Dt} + \nabla \cdot (k\, \nabla T) + \phi \tag{3}$$

$$\phi = (\bar{\bar{\tau}} \cdot \nabla)\vec{V} = \tau_{ij} \frac{\partial V_i}{\partial x_j} \tag{4}$$

2.6 Boundary Conditions

As the fan has a specific angular velocity and different air flow velocity were applied, these criteria were put into consideration for boundary conditions. In the cell zones, mesh motion was applied to fan body and as per the product data sheet angular velocity of 4600 rpm was applied. For inlet boundary, air flow velocity ranging from 2.5 to 7.5 m/s was applied for different cases. For outlet boundary, the gauge pressure was kept at zero pascal. Also, the wall zones were kept stationary. Temperature for the whole geometry was kept at 300k as initial condition.

3. Results and Discussion

To measure the performance of an axial fan, static pressure, total pressure, flow rate, rotation speed, motor input, mechanical efficiency etc. parameters are required. Among them static pressure and flow rate are most important to characterize the performance.

As for the inlet boundary condition, three different air flow velocity were applied, and results were analyzed accordingly. A side-by-side comparison was done for both the blades of different inlet velocity. Static pressure limit was checked for all the cases and maximum velocity was determined.

3.1 Velocity 2.5 m/s

For air flow velocity 2.5 m/s , both the fans experienced static pressure below the allowable limit. For five blade fan, the maximum static pressure was 5.58 Pa(Figure 3a) while for seven blade fan, it was higher, 5.97 Pa(Figure 3b). The maximum velocity for five blade fan is 3.679 m/s (Figure 4a) while it is 3.784 m/s for the seven blade fan (Figure 4b).

(a) (b)

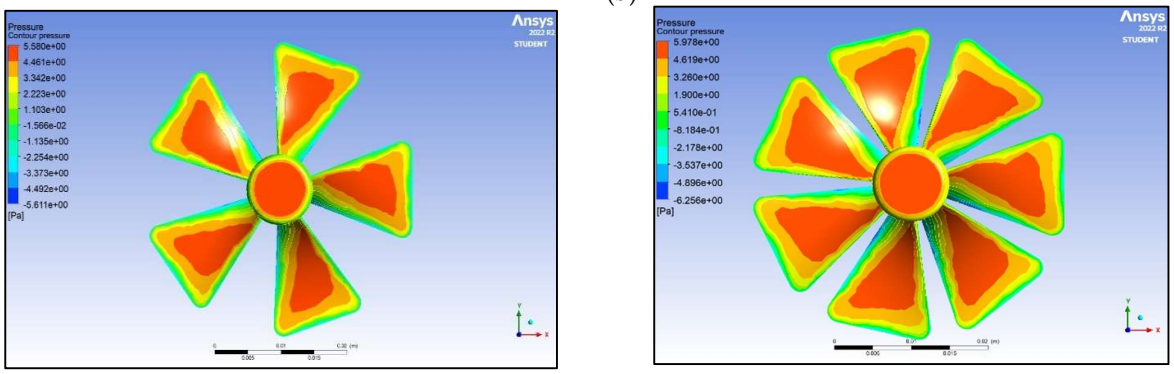

Figure 3. Static Pressure Contour at 2.5 m/s velocity: (a) Five blade axial fan, (b) seven blade axial fan.

(a) (b)

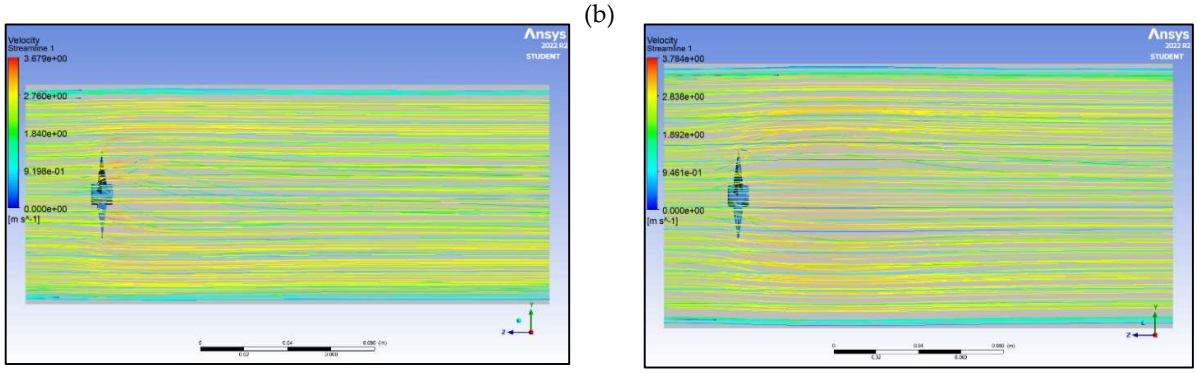

Figure 4. Velocity Streamline at 2.5 m/s velocity: (a) five blade (b) seven blade fan.

3.2 Velocity 5.0 m/s

In this case, air flow velocity for inlet was 5 m/s . The static pressure increased for both fans, but it did not exceed the allowable static pressure limit. While the maximum static pressure for five blade fan was 21.98 Pa(Figure 5c), it was 23.77 Pa for seven blade fan(Figure 5d). In case of velocity, the maximum velocity magnitude increased by almost 50% for both the fans. The maximum velocity for seven blade fan was 7.653 m/s (Figure 5a),while it was 7.241 m/s for five blade fan (Figure 5b).

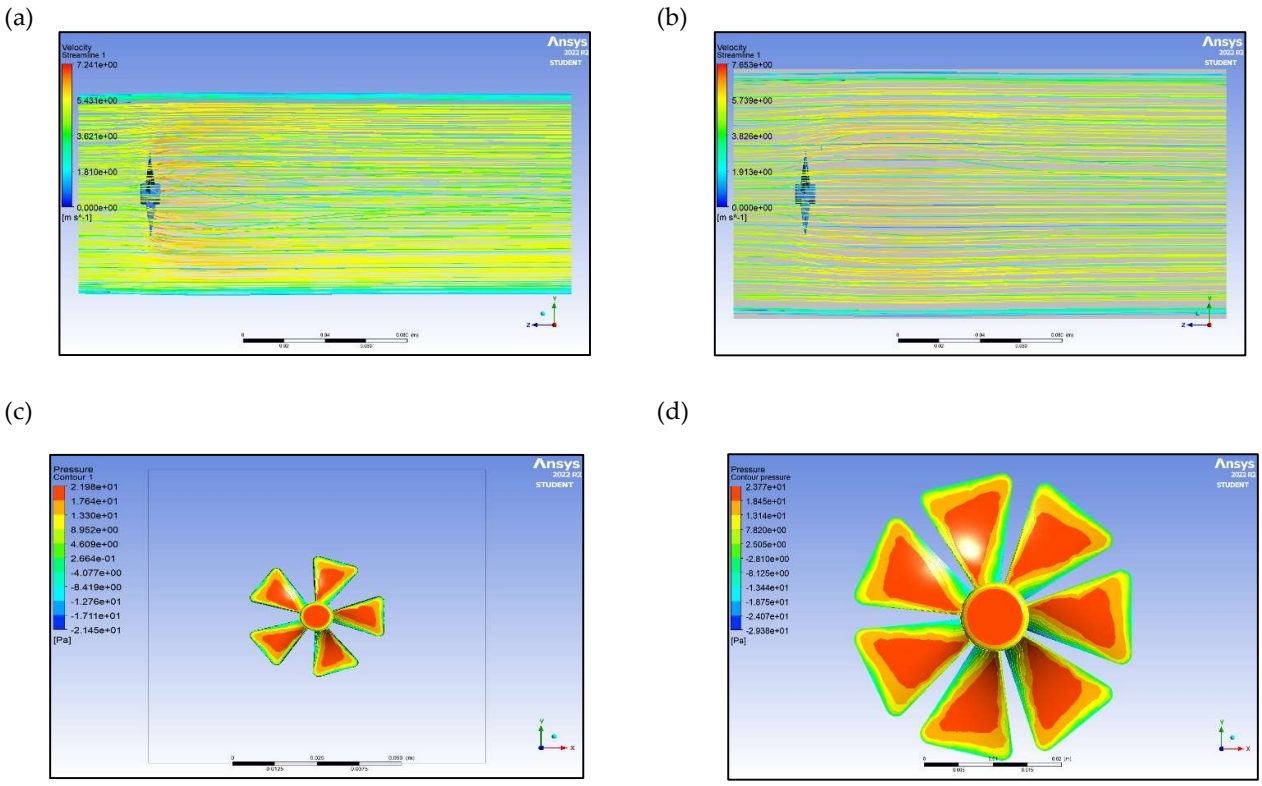

Figure 5. Velocity Streamline at 5 m/s velocity: (a) five blade, (b) seven blade fan. Static Pressure Contour at.5.0 m/s velocity: (c) Five blade axial fan, (d) seven blade axial fan.

3.3 Velocity 7.5 m/s

The static pressure exceeded the limit for air flow inlet velocity 7.5 m/s . Therefore, airflow over 5 m/s velocity would cause deterioration to fan working condition. Here, the maximum static pressure for five blade fan was 48.91 Pa(Figure 6a) and 53.65 Pa for seven blade fan(Figure 6b). The maximum velocity magnitude was 13.27 m/s for five blade fan(Figure 6c), which is higher than the seven blade fan at 13.15 m/s (Figure 6d). Although the velocity was not significantly higher, it was an exception from the previous cases.

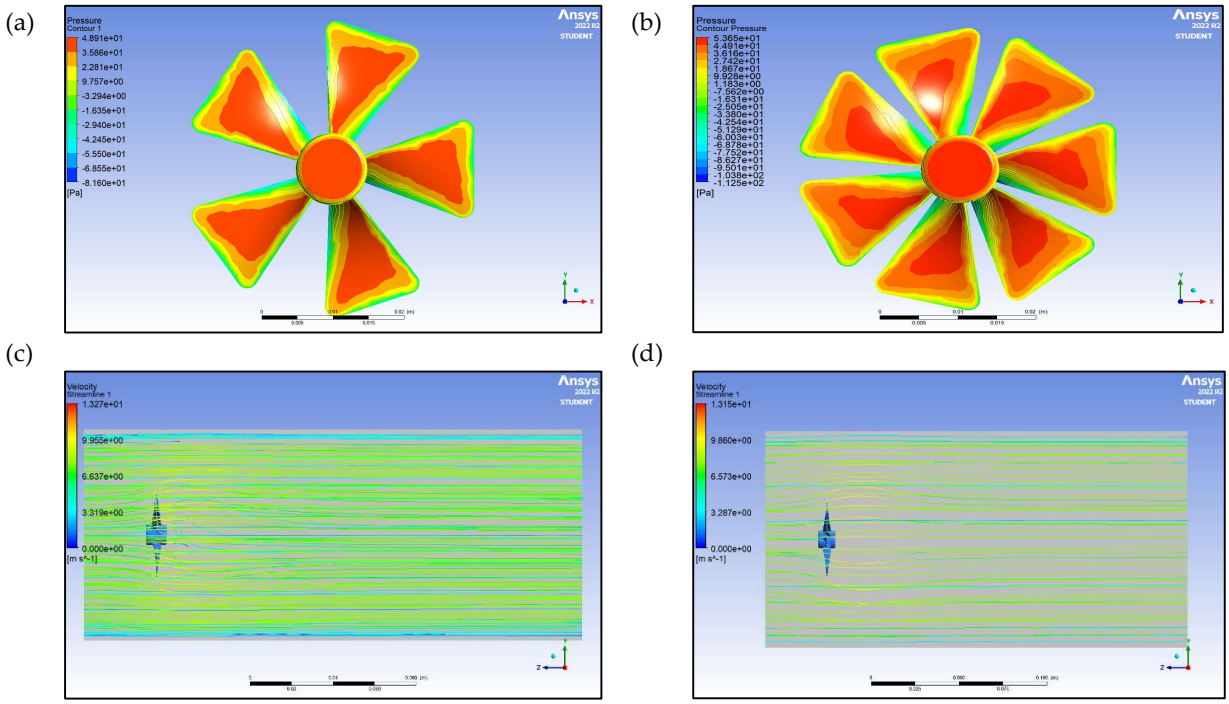

Figure 6. Static Pressure Contour at 7.5 m/s velocity (a) Five blade axial fan, (b) seven blade axial fan. Velocity Streamline at 7.5 m/s velocity: (c) five blade fan, (d) seven blade fan.

3.4 Discussion

From all the cases, some common characteristics were observed. The static pressure was close to zero or lower than zero along the blade edges. But in the mid part of the blade and close to vicinity of the center, pressure increased, and maximum pressure was observed there. It happened in all cases. The maximum static pressure was observed from inlet to the front portion of the blades while the negative pressure zone was observed mostly in the backside of the blades. In case of velocity streamline plots, maximum velocity flow was observed close to fan blades. But as the distance from fan body increased, the velocity of flow began to decrease and turned into a uniform flow. It was applicable for all the cases.

With the increase, inlet flow velocity, static pressure increased for both the fans. The maximum allowable static pressure was 23.77 Pa, which was for seven blade fan at 5 m/s inlet air flow velocity. But at 7.5 m/s velocity static pressure was significantly higher than the allowable maximum static pressure of 24.909 Pa for both the fans.

For all the cases, static pressure of seven blade fan was higher compared to the five-blade fan. But the difference was not that significant. As the fans were operating at a remarkably high angular velocity and the dimension of the fans and domain were small, that is why the static pressure difference was not significant.

Maximum velocity was always higher for seven blade fan than the five blade fan. But, for 7.5 m/s inlet air flow velocity five blade fan experienced the higher velocity. The difference between maximum velocity magnitudes were not significant, due to smaller domain and high operating angular velocity of the fans.

4. Conclusion

This study revealed that increasing blade number from five to seven enhances static pressure generation, though the performance difference remains modest under the tested conditions. Both fan configurations performed within acceptable limits at inlet velocities up to 5 m/s; however, operation at 7.5 m/s caused static pressure to exceed the allowable limit, indicating a potential risk of performance degradation at higher flow rates. The study was constrained by simplified geometry assumptions and lacked experimental validation. Future investigations should incorporate experimental investigation to validate the simulation results, extend the analysis to additional blade configurations, and examine the effects of blade angle variations and efficiency characteristics for comprehensive fan optimization.

References

1. Bleier, F.P. *Fan Handbook: Selection, Application, and Design*; McGraw-Hill, 2018;
2. Kumawat, H. Modeling and Simulation of Axial Fan Using CFD. **2014**, *8*.
3. Liu, S.H.; Huang, R.F.; Chen, L.J. Performance and Inter-Blade Flow of Axial Flow Fans with Different Blade Angles of Attack. *J. Chin. Inst. Eng.* **2011**, *34*, 141–153, doi:10.1080/02533839.2011.553032.
4. Liu, R.; Xu, S.; Sun, K.; Ju, X.; Zhang, W.; Wang, W.; Ma, X.; Pan, Y.; Li, J.; Ren, G. CFD Analysis and Optimization of Axial Flow Fans. *Int. J. Simul. Multidiscip. Des. Optim.* **2024**, *15*, 11, doi:10.1051/smdo/2024007.
5. Podgaietsky, G.L.; Ronzoni, A.F.; Hermes, C.J.L. A Model-Based Design Approach for Low-Pressure Axial Fan Blades Considering the Air Flow System Characteristics. *Int. J. Refrig.* **2024**, *168*, 484–491, doi:10.1016/j.ijrefrig.2024.09.003.
6. Panigrahi, D.C.; Mishra, D.P. CFD Simulations for the Selection of an Appropriate Blade Profile for Improving Energy Efficiency in Axial Flow Mine Ventilation Fans. *J. Sustain. Min.* **2014**, *13*, 15–21, doi:10.7424/jsm140104.
7. Patankar, S.V.; Spalding, D.B. A Calculation Procedure for Heat, Mass and Momentum Transfer in Three-Dimensional Parabolic Flows. In *Numerical prediction of flow, heat transfer, turbulence and combustion*; Elsevier, 1983; pp. 54–73.
8. Van Doormaal, J.P.; Raithby, G.D. Enhancements of the Simple Method for Predicting Incompressible Fluid Flows. *Numer. Heat Transf.* **1984**, *7*, 147–163, doi:10.1080/01495728408961817.
9. Razib, R.; Hasan, M.; Bhuiyan, S.A.; Kader, M.S. Numerical Analysis of Steady Laminar Flow by Finite Volume Method in Connection with Simple Algorithm. In Proceedings of the Proceedings of the 13th International Conference on Marine Technology (MARTEC 2022); 2023.
10. Ocker, C.; Czwielong, F.; Chaitanya, P.; Pannert, W.; Becker, S. Aerodynamic and Aeroacoustic Properties of Axial Fan Blades with Slitted Leading Edges. *Acta Acust.* **2022**, *6*, 48.
11. Qi, W.C.; Cheng, K.; Li, P.C.; Li, J.Y. Enhancing Axial Fan Noise Reduction through Innovative Wavy Blade Configurations. *J. Appl. Fluid Mech.* **2024**, *17*, 1430–1443.
12. Thumbe, J.; Jyothish, V. Analysis of Six Bladed Axial Fan Using ANSYS. *Int J Eng Res Manag Stud* **2017**, 68–75.
13. RS PRO Axial Fan, 5 V Dc, DC Operation, 16.9m^3/h, 750mW, 50 x 50 x 10mm | RS Available online: https://my.rs-online.com/web/p/axial-fans/1442047 (accessed on 6 January 2023).
14. Versteeg, H.K. *An Introduction to Computational Fluid Dynamics the Finite Volume Method, 2/E*; Pearson Education India, 2007;
15. Shih, T.-H.; Liou, W.W.; Shabbir, A.; Yang, Z.; Zhu, J. A New *k*-ϵ Eddy Viscosity Model for High Reynolds Number Turbulent Flows. *Comput. Fluids* **1995**, *24*, 227–238, doi:10.1016/0045-7930(94)00032-T.

Funding: This research received no external funding

Conflicts of Interest: The author declares no conflict of interest.